Article

Cell Reports

Meiotic Nuclear Oscillations Are Necessary to Avoid Excessive Chromosome Associations

Graphical Abstract

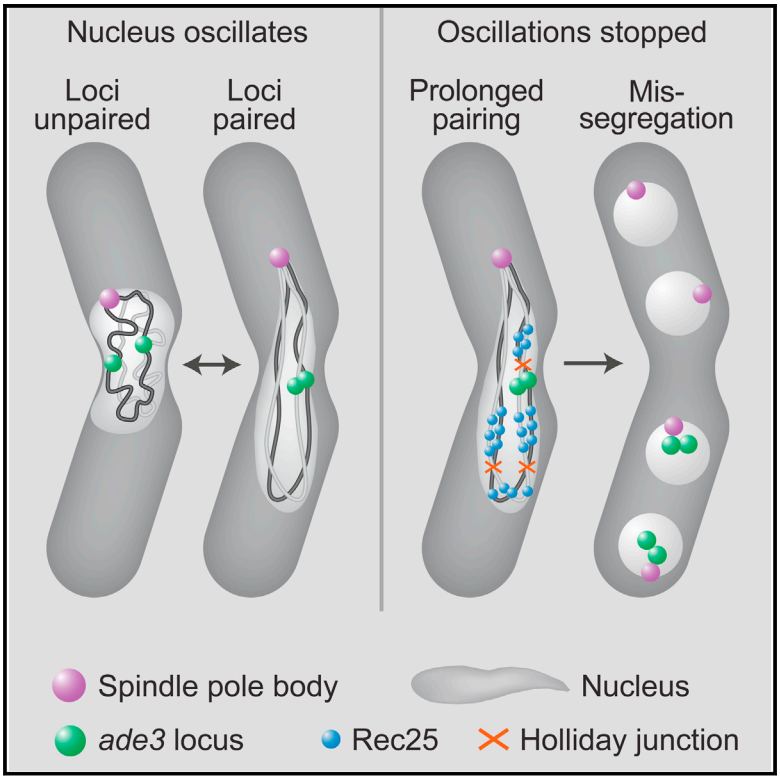

Authors

Mariola R. Chacón, Petrina Delivani, Iva M. Tolić

Correspondence

tolic@irb.hr

In Brief

Chacón et al. find that meiotic nuclear oscillations have a dual role in chromosome dynamics. They enable proper spatial alignment of homologous chromosomes for their initial pairing and favor pairing/unpairing dynamics that prevent excessive chromosome connections and mis-segregation.

Highlights

- Nuclear oscillations promote the dynamics of homologous loci in meiotic prophase
- The first pairing events of homologous loci require nuclear movement
- Prolonged chromosome pairing is accompanied by mis-segregation
- Mis-segregation is rescued by Mus81 overexpression

Chacón et al., 2016, Cell Reports *17*, 1632–1645
November 1, 2016
http://dx.doi.org/10.1016/j.celrep.2016.10.014

CellPress

OPEN ACCESS
CellPress

Cell Reports
Article

Meiotic Nuclear Oscillations Are Necessary to Avoid Excessive Chromosome Associations

Mariola R. Chacón,[1,3,4] Petrina Delivani,[1,3] and Iva M. Tolić[1,2,5,*]
[1]Max Planck Institute of Molecular Cell Biology and Genetics, Pfotenhauerstrasse 108, 01307 Dresden, Germany
[2]Ruđer Bošković Institute, Bijenička Cesta 54, 10000 Zagreb, Croatia
[3]Co-first author
[4]Present address: Institute of Physiological Chemistry, Faculty of Medicine Carl Gustav Carus, Dresden University of Technology, Fiedlerstrasse 42, MTZ, 01307 Dresden, Germany
[5]Lead Contact
*Correspondence: tolic@irb.hr
http://dx.doi.org/10.1016/j.celrep.2016.10.014

SUMMARY

Pairing of homologous chromosomes is a crucial step in meiosis, which in fission yeast depends on nuclear oscillations. However, how nuclear oscillations help pairing is unknown. Here, we show that homologous loci typically pair when the spindle pole body is at the cell pole and the nucleus is elongated, whereas they unpair when the spindle pole body is in the cell center and the nucleus is round. Inhibition of oscillations demonstrated that movement is required for initial pairing and that prolonged association of loci leads to mis-segregation. The double-strand break marker Rec25 accumulates in elongated nuclei, indicating that prolonged chromosome stretching triggers recombinatory pathways leading to mis-segregation. Mis-segregation is rescued by overexpression of the Holliday junction resolvase Mus81, suggesting that prolonged pairing results in irresolvable recombination intermediates. We conclude that nuclear oscillations exhibit a dual role, promoting initial pairing and restricting the time of chromosome associations to ensure proper segregation.

INTRODUCTION

At the onset of meiosis, in most eukaryotes, homologous chromosomes are not associated. Consequently, homologous chromosomes execute a search process to detect each other and stabilize chromosome pairs. Movement of chromosomes has been suggested as the main mechanism of homology search, since the abrogation of movement led to the loss of chromosome pairing and recombination (Ding et al., 2004, 2007; Labrador et al., 2013; Parvinen and Söderström, 1976; Phillips et al., 2009; Sato et al., 2009; Scherthan et al., 2007; Woglar and Jantsch, 2014; Wynne et al., 2012; Yamamoto et al., 1999). A recent theoretical work has shown that the viscous drag experienced by the chromosomes due to their movement can align homologous chromosomes (Lin et al., 2015). However, it has been proposed that chromosome movement also might play other roles in meiosis (Koszul and Kleckner, 2009), such as that extensive movements during meiotic prophase are required to resolve homologous entanglements or non-homologous connections (Conrad et al., 2008; Koszul et al., 2008; Woglar et al., 2013). To date it remains unclear as to what role can be attributed to the nuclear movement in the process of homologous chromosome pairing.

To establish chromosome movement in most eukaryotes, telomere ends of chromosomes associate with the nuclear envelope to form a bouquet. Formation of the bouquet is a prerequisite for chromosome alignment, pairing, and recombination (Chikashige et al., 1994, 2006; Horn et al., 2013; Scherthan, 2001; Smith et al., 2001; Tomita and Cooper, 2006). Once chromosomes are aligned, they have to establish a stable connection, which consists of physical links built up by the synaptonemal complex and chiasmata (Libuda et al., 2013; Loidl, 2006). Subsequently, the chiasmata are resolved into crossovers in order to segregate homologous chromosomes and provide genetic diversity (Villeneuve and Hillers, 2001).

The molecular mechanism behind the formation of chiasmata involves double-strand breaks (DSBs) by Spo11 (Rec12 in fission yeast), a type II topoisomerase-like protein (Keeney et al., 1997). DSBs give rise to single-stranded DNA, which invades the DNA duplex of the homologous partner, and may result in Holliday junctions after repair. Holliday junctions in turn have to be resolved by the action of resolvases to form crossovers (O'Neil et al., 2013; Smith et al., 2001). The number of DSBs is precisely regulated by specific regulatory mechanisms that turn off DSB formation (Rosu et al., 2013).

The fission yeast *Schizosaccharomyces pombe* displays a meiotic prophase that is characterized by an extensive nuclear movement, where chromosomes are led by all the telomeres clustered at the spindle pole body (SPB, the centrosome equivalent) in a bouquet formation (Chikashige et al., 1994). The SPB is located at the leading edge of the nucleus and oscillates back and forth along the cell axis, moving continuously between the two ends of the cell for roughly 2 hr prior to the meiotic divisions (Figure 1A; Movie S1) (Ding et al., 1998). This movement is driven by pulling forces exerted by the combination of dynein motors attached to anchor proteins in the cortex and microtubules (Ananthanarayanan et al., 2013; Vogel et al., 2009; Yamamoto et al., 1999). Mutation of dynein heavy chain in fission yeast

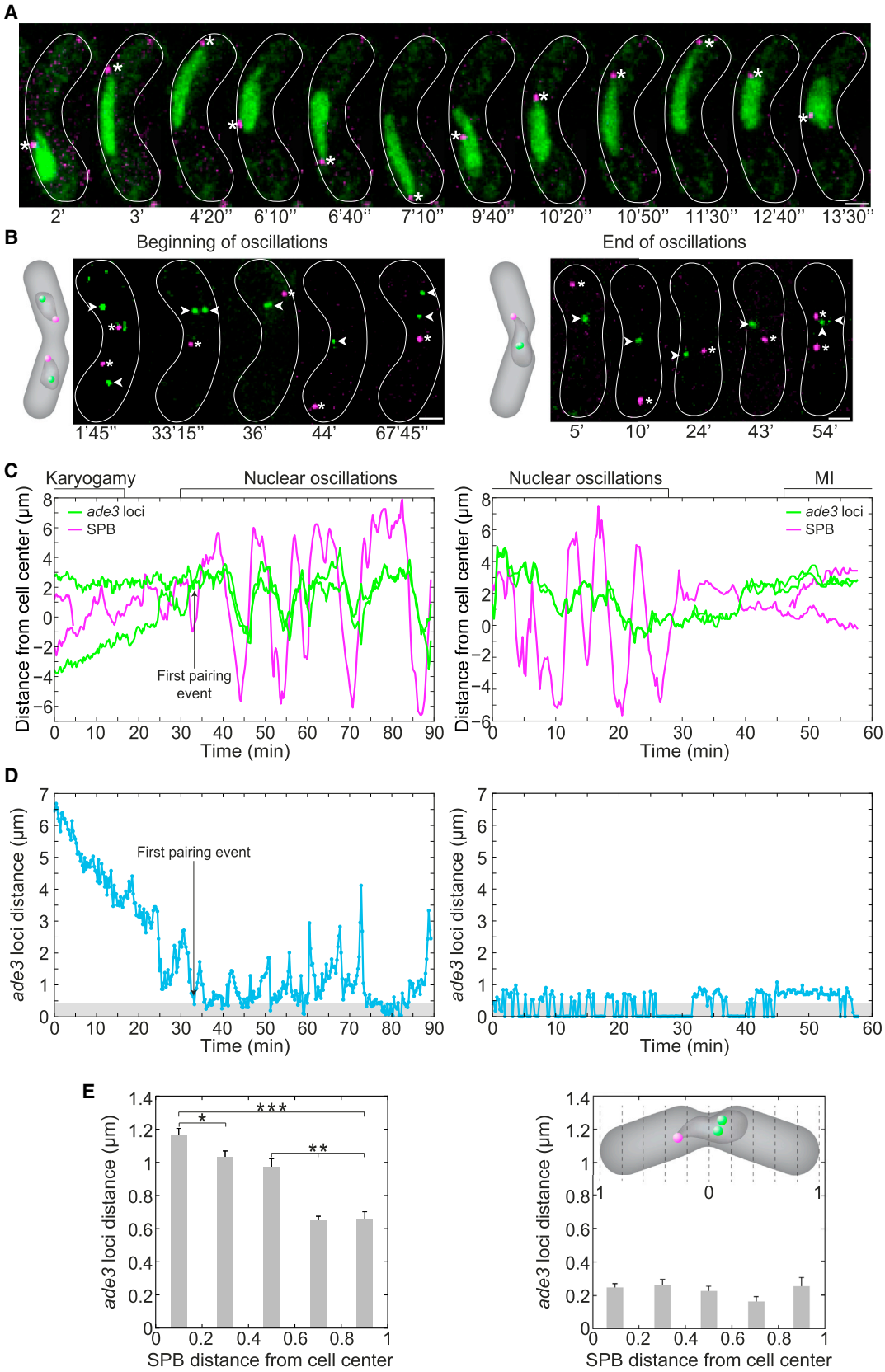

(legend on next page)

abolishes nuclear movement during meiotic prophase and results in unpaired chromosomes and reduced recombination (Ding et al., 2004; Yamamoto et al., 1999). An additional feature of meiosis in fission yeast is the presence of linear elements (LinEs) instead of the synaptonemal complex and the absence of crossover interference (Bähler et al., 1993; Munz, 1994), making it an excellent model for examining the effect of nuclear movement on chromosome dynamics.

Here, we study the role of nuclear oscillations on chromosome dynamics during meiotic prophase in fission yeast. We show a correlation between the SPB position and the distance between the labeled *ade3* loci, which are on the long arm of chromosome I (Ding et al., 2004). We observed that elongation and rounding of the nucleus during its oscillations promote chromosome pairing and unpairing, respectively. We inhibited nuclear oscillations at different time points of meiotic prophase, and we demonstrated that movement is required for (1) the initial pairing of homologous loci and (2) to avoid excessive chromosome associations, which lead to mis-segregation. Furthermore, we observed that chromosome configuration in an elongated nucleus promoted accumulation of the LinE component Rec25, which could in turn promote recombinatory pathways, leading to the accumulation of irresolvable recombination intermediates at the end of meiotic prophase. Moreover, the mis-segregation phenotype was rescued by overexpression of the Holliday junction resolvase Mus81. We propose a dual role of nuclear oscillations in chromosome dynamics: pairing homologous chromosomes through stretching of the nucleus at the beginning of nuclear oscillations and unpairing the chromosomes via constant changes of the nuclear shape throughout the oscillations, to guarantee proper segregation.

RESULTS

Pairing of Homologous Loci Is Correlated with the Spindle Pole Body Position

To elucidate the role of nuclear oscillations during meiotic prophase, we studied the dynamics of homologous chromosomes in *Schizosaccharomyces pombe*. We performed time-lapse experiments in fission yeast zygotes in which the *ade3* locus on chromosome I was labeled with GFP via the lacO/lacI reporter system and served as a probe for chromosome interactions (Ding et al., 2004). We chose this locus because it is situated in the central region of the longer arm of the longest chromosome; hence, it is far away from the telomere and from the centromere. In the same strain, the SPB was labeled by tagging one component (Sid4) with mCherry to follow the SPB oscillations throughout meiosis (strain PD13, see Experimental Procedures and Table S1). The SPB and the *ade3* loci were tracked automatically by using our recently developed tracking software (Krull et al., 2014). We observed that the loci paired and unpaired depending on the position of the SPB and that there was a correlation between SPB position and that of both loci (Figures S1A and S1B). The loci distance decreased, on average, over time during the whole process of meiotic prophase, consistent with previous observations (Ding et al., 2004) (Figure S1C). We defined homologous loci as being paired when the distance between the center of GFP signals was smaller than 400 nm, similar to Ding et al. (2004).

Interestingly, we observed that the movement of the *ade3* loci was correlated with the movement of the SPB at the beginning of the oscillations, but not at the end (Figures 1B and 1C; Movie S2). During the first several periods of the oscillations, while the SPB moved toward one cell pole, the *ade3* loci also moved toward that pole, which was accompanied by a decrease in distance between the loci (Figures 1B–1D, left). The average distance between the *ade3* loci was smaller when the SPB was close to the cell pole than when it was in the central region of the cell (Figure 1E, left). During the last several periods of the oscillations, on the contrary, the *ade3* loci were paired most of the time and their average distance was smaller than 400 nm, irrespective of the position of the SPB (Figures 1B–1E, right).

To examine the behavior of a locus at a different position on the chromosome, we followed the centromere-proximal *cen2* locus on chromosome II (Figure S1D; strains AK03 and AK04 in Table S1). We found that, during the first several periods of the oscillations, the distance between the *cen2* loci was smaller when the SPB was close to the cell pole than in the central

Figure 1. Pairing of *ade3* Loci Is Correlated with the Spindle Pole Body Position

(A) Time-lapse experiments of zygotes expressing Rec8-GFP (DNA marker in green) and Sid4-mCherry (SPB marker in magenta, asterisk). Note that the nucleus alternates between round and elongated shapes during the oscillations depending on the SPB position.

(B) Scheme and images of zygotes showing the *ade3* locus tagged with GFP (green, white arrowheads) and the SPB as shown in (A) (magenta, asterisk) during the beginning (left, beginning of oscillations) and the end (right, end of oscillations) of nuclear oscillations. After karyogamy (beginning of oscillations, 1 min 45 s and 33 min 15 s), the *ade3* loci pair when the SPB goes to the cell pole (36 and 44 min) and unpair (67 min 45 s) when the SPB passes the cell center. In the panel on the right (end of oscillations), at 54 min the zygote proceeds to meiosis I (strain PD13, see Table S1). In (A) and (B), images were acquired with an interval time of 10–15 s between images. Numbers below the pictures indicate the time in minutes (′) and seconds (″), and the white lines mark the cell outline. Scale bar, 2 μm.

(C) Plot of *ade3* loci and SPB position as a function of time (green and magenta lines, respectively) during the beginning (left) and the end (right graph) of nuclear oscillations corresponding to the cells shown in (B). The *ade3* loci follow the movement of the SPB. The black arrow indicates the first pairing. Nuclear oscillations started 19.96 ± 9.12 min after the two SPBs fused (n = 7 cells). We considered that oscillations had started after the SPB moved on the long axis for at least 25% of the highest amplitude of the oscillation.

(D) Plot (corresponding to the cells in B) of distance of *ade3* loci as a function of time during the beginning (left graph) and the end (right graph) of nuclear oscillations. The gray area indicates the defined pairing distance (400 nm). The black arrow indicates the first pairing event. The first pairing event lasted for 20.63 ± 11.16 s and was observed only after the oscillations had started in ten of 11 cells. The last contact was typically 4 ± 1.77 min (n = 6 cells). The duration of the pairing (mean ± SD) at the beginning of the oscillations was 9.31 ± 4.41 min during the first hour and at the end 18.94 ± 2.40 min during the last half hour (n = 17 cells). We considered that oscillations finished when the SPB moved on the long axis less than 25% of the highest amplitude.

(E) Quantification of distance between *ade3* loci (mean ± SD) versus the SPB position (scheme inside plot on the right) during the first (plot on left) and last (plot on right) five oscillations until meiosis I is shown (n = 2,011 data points from 17 cells from ten different experiments; ANOVA test, * $0.01 < p < 0.05$, ** $0.001 < p < 0.01$, and *** $p < 0.001$; $p_{\text{cell pole (I, last bar) and cell center (0, first bar)}} = 5*10^{-15}$, ANOVA test).

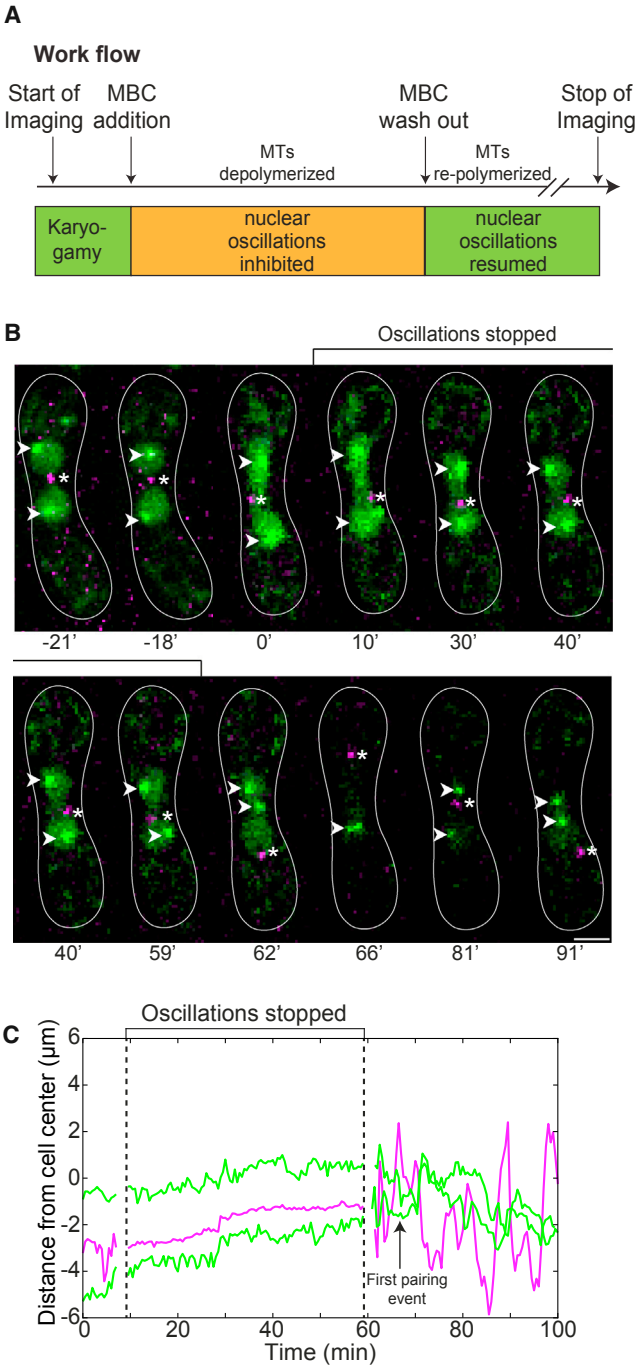

Figure 2. First Pairing of Homologous Loci Requires Nuclear Movement

(A) Work flow of the experiments where nuclear oscillations were abrogated by adding the MT-depolymerizing drug MBC is shown (see the Experimental Procedures).

(B and C) PD13 zygote treated with MBC after karyogamy to inhibit the beginning of nuclear oscillations (B) and plot of the SPB and loci positions over time (C). Note that two separate nuclei can be distinguished by the dark space (no lacI-GFP signal) between them at −21 and −18 min (B). We acquired time-lapse images of each cell, and we considered that karyogamy was completed when small movements of the SPB and a shared region of a continuous GFP signal throughout both nuclei was seen, indicating that the nuclei had fused. Note that the first pairing, i.e., the first time the distance between the loci decreased below 400 nm (B, 66 min, and C, black arrowhead) does not occur until the oscillations start. Images were acquired each 30 s. Time is given in minutes. The white line in the image marks the cell outline. Scale bar, 2 μm. Representative images and graph of four experiments with five cells are shown.

part of the cell, but the difference was not statistically significant (Figure S1D, left). Similar to *ade3* loci, during the last several periods of the oscillations, the *cen2* loci were paired most of the time and their average distance was smaller than 400 nm, irrespective of the position of the SPB (Figure S1D, right).

To examine the dynamics of heterologous loci, we followed the *ade3* locus on the arm of chromosome I and the *cut3* locus on the arm of chromosome II (Figure S1E; strains PD05 and PD14 in Table S1, see the Experimental Procedures). Similar to the homologous *ade3* loci, the distance between the heterologous *ade3* and *cut3* loci was smaller when the SPB was close to the cell pole than in the central part of the cell, during the first several periods of the oscillations (Figure S1E, left). However, contrary to the homologous loci, the heterologous loci remained separated at the end of the oscillations, with an average distance between the loci larger than 400 nm. During the last several periods of the oscillations, the heterologous loci showed a similar behavior as in the beginning of the oscillations, insofar as the distance between the heterologous loci was smaller when the SPB was close to the cell pole than in the central part of the cell (Figure S1E, right).

Based on these results, we conclude that nuclear oscillations promote the dynamics of homologous loci in such a way that the loci approach each other when the SPB is close to the cell pole, whereas the loci move apart when the SPB passes through the central part of the cell. This correlation is lost at the end of the oscillations when the homologous loci are predominantly paired. Heterologous loci show this correlation throughout the oscillations, as they do not undergo stable pairing.

Initial Pairing of Homologous Loci Requires Nuclear Oscillations

Next, we asked whether the pairing of *ade3* loci requires nuclear movement. In Figure 1B, it can be seen that before karyogamy and the fusion of the two SPBs, the loci were separated in the two poles of the zygote. Nuclear oscillations commenced roughly 20 min after the fusion of the two SPBs (n = 7 cells). However, only after the oscillations had started was the pairing of the loci observed for the first time (n = 10 of 11 cells, Figures 1C and 1D, first pairing event; see also Table S2 for statistics).

To test whether the first pairing requires nuclear oscillations, we inhibited oscillations by using a microtubule-depolymerizing agent methyl benzimidazol-2-yl-carbamate (MBC) (Carbendazim, see Figure 2A and the Experimental Procedures). We added MBC to zygotes that had already undergone karyogamy and had fused SPBs and nucleoplasm but that had not yet paired *ade3* loci (Figure 2B; Movie S1). We saw that, as long as nuclear oscillations were inhibited by MBC, homologous *ade3* loci did not come into close proximity (n = 5 cells). The SPB did not move and the loci remained well separated with a distance of 2–4 μm

between them (Figure 2C). Only after MBC was washed out did the SPB resume its movement along the axis of the zygote and the first pairing event occurred. Immediately after one full oscillation period of the nucleus, the distance between the labeled loci decreased and they paired (Figure 2C, arrow). Based on these results, we conclude that the first pairing events of homologous *ade3* loci require SPB movement.

Nuclear Oscillations Promote *ade3* Loci Dynamics

At the beginning of the meiotic prophase, a few nuclear movements back and forth were sufficient to bring the two homologous loci into close proximity, but the nuclear oscillations continued. Thus, the question remained, what is the role of nuclear oscillations after the first pairing has occurred?

We set out to study the effect of stopping the oscillations when the *ade3* loci were paired versus unpaired. We induced meiosis and added MBC after five to seven oscillations. Following this inhibition, we resumed oscillations by washing out MBC. The cells in which during the MBC treatment the SPB was close to the cell pole (i.e., more than 20% of the cell half-length away from the cell center) were designated as those with paired loci, whereas the cells in which the SPB was close to the cell center (i.e., less than 20% of the cell half-length away from the cell center) were designated as those with unpaired loci, based on the data from Figure 1E. Indeed, the average distance between the *ade3* loci was smaller throughout the MBC treatment in the loci paired versus loci unpaired group (Figures S2A and S2B). Even though the SPB moved slightly toward the cell center during MBC treatment, its distance from the cell center, as well as its distance from the loci, was larger throughout the MBC treatment in the cells with paired loci than in those with unpaired loci (Figure S2A).

Strikingly, in the population of cells in which *ade3* loci were paired during the time when the oscillations were stopped, the loci typically did not unpair anymore after the resumption of oscillations (Figures 3A, 3C, and 3D; Movie S3). Despite the resumed nuclear oscillations, indicated by the movement of the SPB (Figures 3A and S2C), paired loci stayed paired for at least 50 min (n = 6 cells, Figure 3C). For comparison, in untreated cells pairing of the loci for such a long time was not observed (n = 7 cells, Figure S2E) (Ding et al., 2004).

In the second population of cells, *ade3* loci were unpaired when the nuclear movement was stopped by using MBC (Figure 3B). In contrast to the first population, the loci resumed normal dynamics of pairing and unpairing after the oscillations restarted, indicated by the movement of the SPB (n = 6 cells, Figures 3B–3D and S2D). Taken together, these results suggest that oscillations promote the dynamics or breathing of the loci, thereby preventing prolonged pairing of chromosomes.

Prolonged Pairing of *ade3* Loci Results in Mis-segregation

Following the observation that prolonged pairing of *ade3* loci when the oscillations were paused led to stable pairing until the end of meiotic prophase, we wanted to test whether this has an effect on chromosome segregation in meiotic divisions. To this end, we stopped oscillations by using MBC and followed the zygotes until the end of meiosis I and II.

Interestingly, we found mis-segregated *ade3* loci at the end of meiosis I and II in the population of cells where oscillations were stopped when the *ade3* loci were paired (Figures 4A, 4C, and 4D). As shown in Figure 4A, the zygote contained mis-segregated loci, identified by the accumulation of the four GFP dots in the vicinity of one SPB in meiosis I and in the vicinity of two of four SPBs in meiosis II (Figure 4A, 250 and 290 min, respectively; Movie S3). Despite the resumption of oscillations of the SPB after MBC washout, paired *ade3* loci were mis-segregated (Figures 4A and 4C). Around 36% (23 of 64) of zygotes in this condition exhibited segregation problems: ten of these 23 cells showed a single unsegregated nucleus with one SPB spot and all the loci in the cell center, whereas the remaining 13 displayed mis-segregation with two to four SPBs and all the loci in one half of the cell (Figure 4E). In contrast, when *ade3* loci were not paired at the moment of MBC addition (Figures 4B–4D), 96% of the zygotes segregated the loci as in untreated cells, with four GFP signals associated with four SPBs (Figures 4B, 4C, and 4E; see Figures S1A, S1B, S3A, and S3B for control cells). These results suggest that prolonged chromosome pairing during meiotic prophase is accompanied by mis-segregation.

To rule out the possibility that mis-segregation was caused by off-target effects of MBC treatment, we repeated the experiments by using another microtubule poison, thiabendazole (TBZ; Experimental Procedures). As in experiments with MBC, we observed chromosome mis-segregation when *ade3* loci were paired, but not when they were unpaired, under TBZ treatment (Figure 4E).

To test whether there is a correlation between the number of nuclear oscillations and mis-segregation, we treated PD13 and PD13C cells (Table S1; Experimental Procedures) with MBC just before the end of the oscillations; i.e, before meiosis I. In this scenario, the SPB was in the center and the loci were predominantly paired (as in Figure 1, end of oscillations). We observed that the SPB duplicated during the treatment but the spindle formed and the two SPBs separated only after removing MBC. Under these conditions, the percentage of cells showing segregation problems increased to 83% (15 of 18 cells). We found again the two populations described in Figure 4E: in this case four of these 15 cells showed a single unsegregated nucleus with one SPB spot and all the loci in the cell center, whereas 11 displayed mis-segregation with two to four SPBs and all the loci in one half of the cell. Four of these 11 cells expressed tubulin-mCherry and the spindle showed normal dynamics (Movie S4), which argues against spindle defects as a cause of mis-segregation. However, we cannot exclude the possibility that the intranuclear microtubule array that emerges from the SPB before meiosis I and re-associates the kinetochores with the SPB (Cojoc et al., 2016; Kakui et al., 2013) was impaired, which might explain why segregation problems occurred more frequently when MBC was added late than early in prophase. Taken together, our results support the idea that movement is necessary to keep the loci breathing even when they are paired. Moreover, our experiments suggest that there is a minimum number of oscillations needed to avoid mis-segregation.

To infer the molecular mechanism underlying the observed mis-segregation, we examined the segregation of the whole DNA mass by quantifying its distribution at meiosis II. We

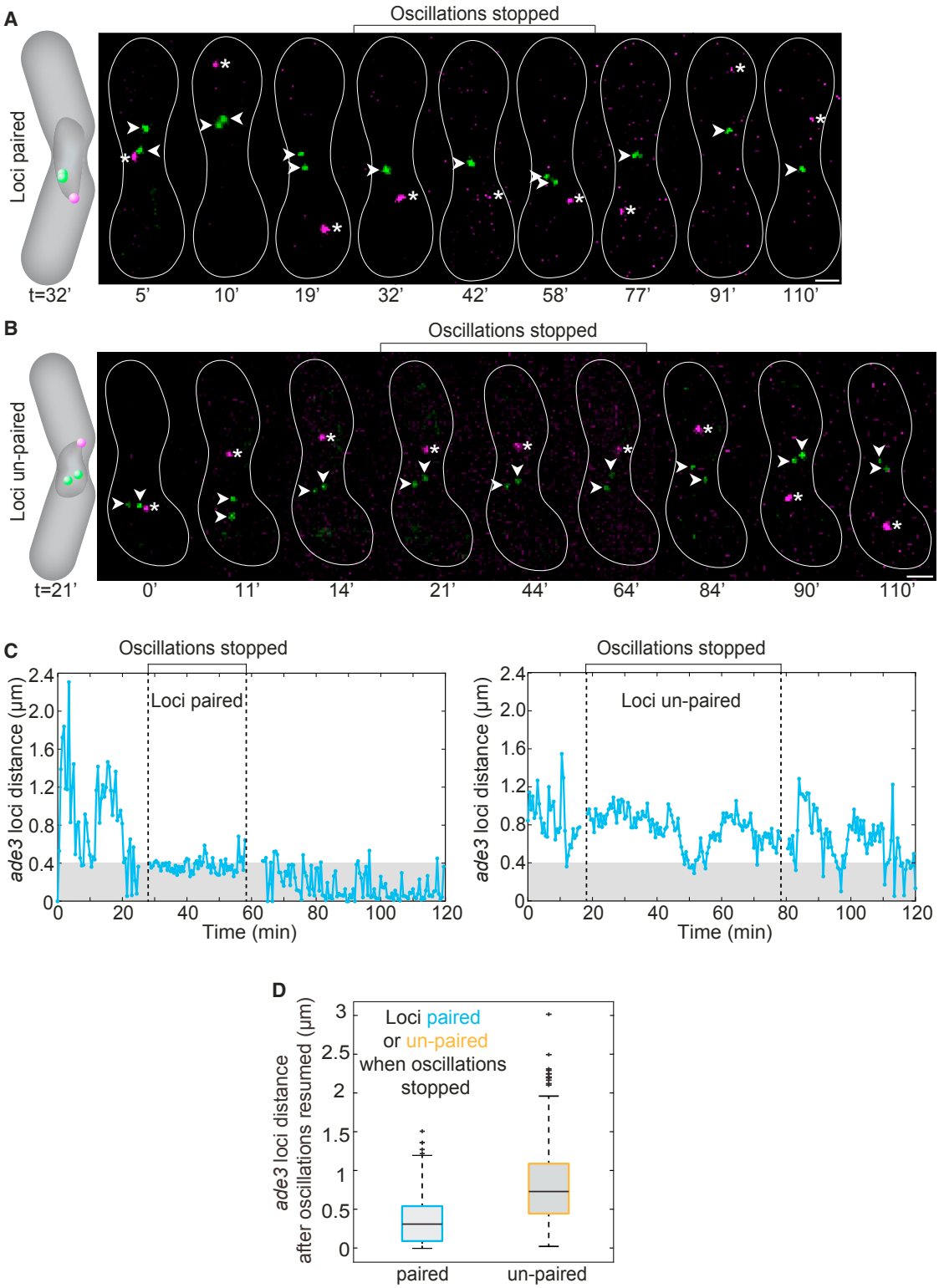

Figure 3. Nuclear Oscillations Promote *ade3* Loci Dynamics

(A and B) Time-lapse images of PD13 zygotes treated with the MT-depolymerizing drug MBC. Nuclear oscillations were stopped when the loci were paired (A) and unpaired (B) (schemes on the left). Before the addition of MBC (up to 19 min in A and 14 min in B), the oscillations occurred normally and the SPB (magenta dot, asterisk) went back and forth from one cell pole to the other and the loci paired and unpaired (green dots, arrowheads). When MBC was added (32–58 min in A and

(legend continued on next page)

hypothesized that the prolonged pairing of the loci is due to production of a class of irresolvable intermediates, which may result from additional initiations of recombination or from failure to mature normally initiated recombination intermediates into a form that can be resolved. When cells have Holliday junctions that cannot be resolved, they fail to segregate the chromosomes correctly in meiosis I, resulting in a single mass of undivided DNA at the end of meiosis II (Boddy et al., 2001). We stained the DNA in living zygotes at meiosis II (Hoechst staining, Experimental Procedures), and we observed a single DNA mass and four SPBs in 70% (n = 10) of the stained zygotes with incorrect segregation, in which the oscillations were stopped by MBC in the configuration of paired *ade3* loci (Figures 4F, top, and S3C). On the contrary, the cells in which the oscillations were stopped in the configuration of unpaired loci displayed four DNA masses associated with four SPBs (Figures 4F, bottom, and S3C), as in untreated cells (Figure S3C). These findings indicate that the mis-segregation observed in our experiments was a result of a failure in segregation in meiosis I, similar to the phenotype described in cells lacking the Holliday junction resolvase Mus81 (Boddy et al., 2001), supporting our hypothesis that prolonged pairing induced by the inhibition of oscillations is accompanied by too many irresolvable recombination intermediates.

Alternatively, formation of a single DNA mass may be due to damage of the meiotic spindle (Tomita and Cooper, 2007; Tomita et al., 2013). To test this possibility, we measured the spindle length and spindle thickness, which is related to the number of microtubules in the spindle, in cells expressing tubulin-mCherry, labeled *ade3* loci, and the SPB (strain PD13C, Table S1 and the Experimental Procedures). The spindle length increased and the thickness decreased in time, with a dynamic that was indistinguishable between untreated cells and those in which the oscillations were stopped by using either MBC or TBZ after washout (Figures S3D and S3E). Moreover, the dynamic was similar in cells in which the oscillations were stopped when *ade3* loci were paired and in those where the loci were unpaired (Figures S3D and S3E). However, mis-segregation was observed primarily in cells where the oscillations were stopped when the loci were paired (Figures S3F and S3G, similar to Figure 4E). These data indicate that the observed mis-segregation was not a consequence of spindle defects in meiosis I.

Our hypothesis that the single DNA mass is due to irresolvable recombination intermediates leads to the prediction that recombination deficiency should convert the single DNA mass (Figure 4F) into four masses with random segregation of the GFP loci. Cells lacking *rec12* displayed from two to four masses of DNA at the end of meiosis II (Figure S3C), consistent with previous work (Sharif et al., 2002). This distribution was different than the one observed in wild-type cells in which the oscillations were stopped when *ade3* loci were paired, which displayed predominantly one mass of DNA when mis-segregated (Figures 4F and S3C). Furthermore, the DNA segregation pattern observed in *rec12* mutant cells in which the oscillations were stopped was similar to that in untreated *rec12* mutant cells (Figure S3C), which was in contrast to the result obtained in wild-type cells (strain PD13, Figure S3C). These findings further support our hypothesis that the mis-segregation following the inhibition of oscillations is due to too many irresolvable recombination intermediates.

Taken together, these results suggest that nuclear movement is required for the proper segregation of homologous chromosomes in meiosis I. We propose that an important role of nuclear oscillations is to move the chromosomes to avoid their prolonged associations, which may lead to irresolvable recombination intermediates, such as unresolved Holliday junctions.

Rec25-GFP Accumulates in Nuclei that Are Stopped in an Elongated Conformation

During meiosis, double-strand breaks lead to the formation of double Holliday junctions, which, when resolved, result in crossovers. We set out to test whether the abrogation of nuclear oscillations affects DSB formation and its downstream pathway. Recently a novel component of the linear elements in fission yeast was described, Rec25, that activates Rec12 to make DSBs, and it is strongly and exclusively enriched at hotspots of DSB formation (Davis et al., 2008; Fowler et al., 2013; Martín-Castellanos et al., 2005). Therefore, we used cells that express Rec25 tagged with GFP (Table S1) as an indirect readout of DSB formation during meiotic prophase (Figures 5A–5D and S4A).

We found that once the oscillations had started, fluorescence intensity of Rec25-GFP increased in the first part of meiotic prophase and decreased at the end of meiotic prophase, as shown in Figures 5A and 5D. GFP signal could not be detected anymore when the oscillations finished (Figure 5A). Similar to Rec8-GFP-expressing cells, cells expressing Rec25-GFP displayed GFP signal in the whole nucleus (compare Figures 1A and 5A), which was confirmed by Hoechst staining of Rec25-GFP-expressing cells (Figure S4A). Thus, Rec25-GFP signal allowed us to monitor the nuclear shape and observe the change from an elongated to a more rounded conformation. In cells expressing Rec8-GFP, we examined the changes in the nuclear shape during the oscillations by measuring the circularity of the nucleus (see the Experimental Procedures). We found that the circularity decreases as the SPB moves away from the cell center; i.e., the nucleus is more elongated when the SPB is near the cell pole and more round when the SPB is near the cell center (Figure S4B). This correlation between the nuclear shape and the SPB position together with the observed relation between the SPB position

21–64 min in B), the oscillations stopped and the SPB and loci were kept at the same position. After washout of MBC, the oscillations resumed, indicated by the movement of the SPB. Images were acquired at a time interval of 30 s. Time is given in minutes. The white lines mark the cell outline. Scale bar, 2 μm.
(C) Plot of *ade3* loci distances over time corresponding to the experiment shown in (A) and (B) (left and right graphs, respectively). The black dashed line indicates the time during which the oscillations were stopped. The gray area indicates the defined pairing distance (400 nm). On the left, the *ade3* loci remained paired after the oscillations resumed, whereas on the right they had normal dynamics (also compare the last three frames in A and B).
(D) Boxplot showing the distribution of the data of *ade3* loci distance after the oscillations resumed in all experiments. The mean distance was 0.34 μm ± 0.08 (n = 281 data points from six cells) when the loci were paired and 0.77 μm ± 0.13 (n = 341 data points from six cells) when the loci were unpaired, from three different experiments (mean ± SD). The difference was statistically significant (p = 0.0002, t test).

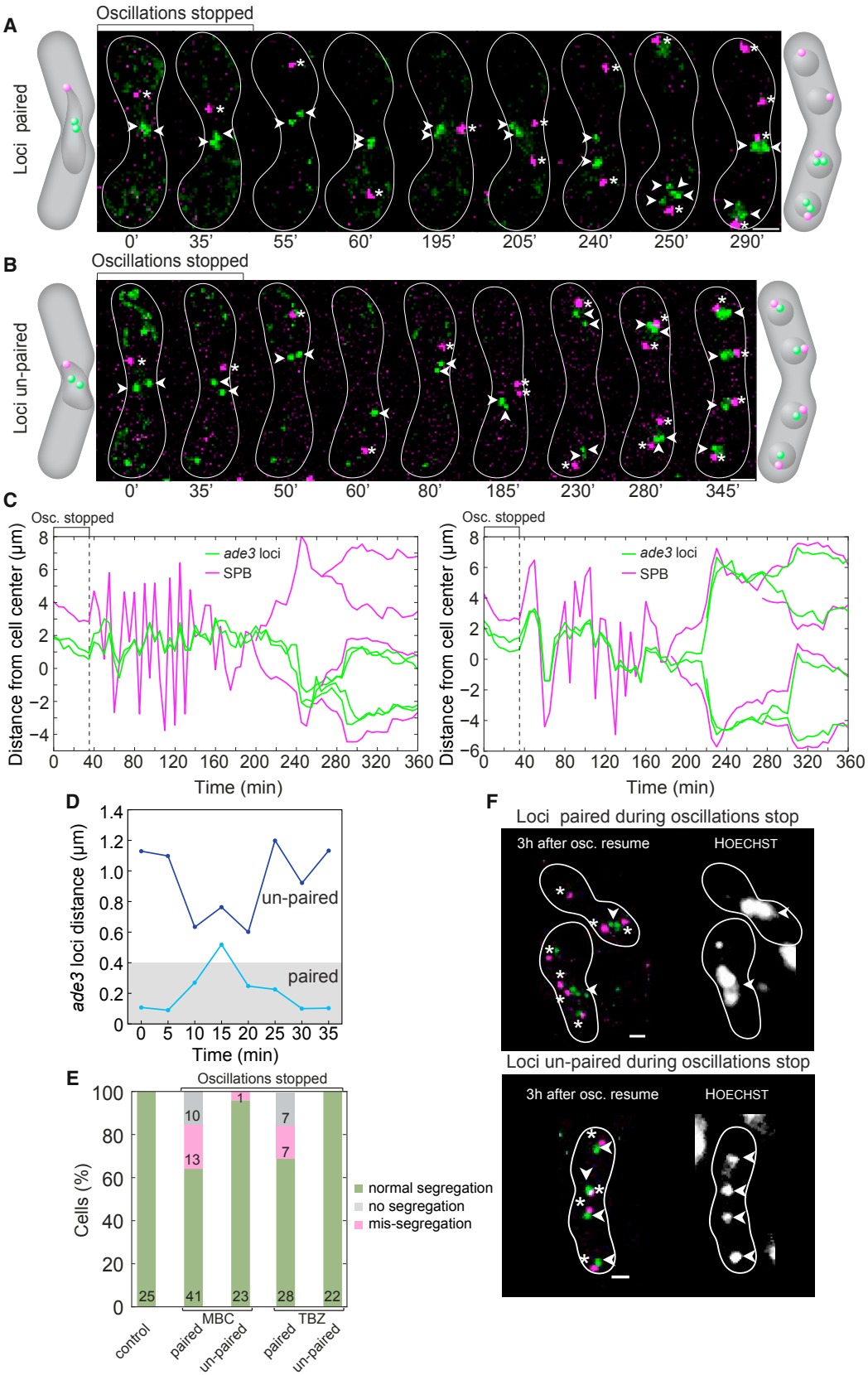

(legend on next page)

and the loci distance (Figure 1E) suggest that the loci are mostly paired when the nucleus is elongated and mostly unpaired when the nucleus is round. In addition, the distance between the SPB and the cell center was similar to the distance between the SPB and *ade3* loci (Figure S2A), which suggests that elongation of the nucleus is accompanied with stretching of the chromosome.

To test whether abrogation of nuclear oscillations has an effect on Rec25-GFP fluorescence, we treated zygotes with MBC and divided the cells into two populations: those that displayed a round nuclear shape and those that displayed an elongated nuclear shape when oscillations were stopped (Figures 5B and 5C). In the first population, the fluorescence intensity of Rec25-GFP in round nuclei behaved as in untreated cells (Figures 5B and 5D). In the second population, on the contrary, the intensity of Rec25-GFP in elongated nuclei increased significantly around 40 min after the addition of MBC (Figures 5C and 5D; Movie S4, second part). Strikingly, this fluorescence intensity remained high until the end of oscillations (Figure 5D). These results indicate that the elongated shape of the nucleus, which is associated with stretched configurations of chromosomes and their paired state, promotes the accumulation of proteins involved in recombination.

Overexpression of the Holliday Junction Resolvase Mus81 Rescues the Mis-segregation that Follows Prolonged Pairing

Finally, to examine whether the observed mis-segregation phenotype is a result of an accumulation of Holliday junctions induced by prolonged pairing when the oscillations are stopped, we overexpressed the Holliday junction resolvase Mus81 by transforming our strain with a plasmid containing Mus81 (strain PD13M81 in Table S1; Experimental Procedures) (Boddy et al., 2001). We treated these cells with MBC and followed paired or unpaired *ade3* loci during meiosis (Figures 5E and 5F). Strikingly, we found that *ade3* loci segregated normally at the end of meiosis, both in the case when the oscillations were stopped when the loci were paired and when the loci were unpaired (Figures 5E–5G). Thus, Holliday junction resolvase rescued the deleterious effects of prolonged chromosome association caused by the abrogation of nuclear oscillations. We conclude that the observed mis-segregation, which was induced by prolonged pairing when the oscillations were stopped, is a result of an accumulation of irresolvable recombination intermediates. Taken together, these observations suggest that the elongated shape of the nucleus and, therefore, stretched chromosome configurations, which promote the association of chromosomes and keep them in close proximity, stimulate increased accumulation of linear element components, eventually triggering an increase in irresolvable recombination intermediate formation through the activation of Rec12 and DSB formation (Figure 5H). These events eventually lead to a failure in segregation in meiosis I.

DISCUSSION

Dual Role of Nuclear Oscillations in Chromosome Dynamics

The mechanism by which homologous chromosomes recognize each other and pair is not known. The combination of an aligned configuration of the chromosomes in a bouquet together with nuclear movement has been proposed to be crucial for chromosomes to pair (Hiraoka and Dernburg, 2009; Scherthan, 2001). However, it is not known if, after karyogamy, the nuclear fusion is sufficient to bring the chromosomes close enough to pair or if the movement is indeed necessary to aid this first recognition. We have shown that the first pairing event requires the nuclear movement.

Figure 4. Nuclear Oscillations Prevent Chromosome Mis-segregation

For a Figure360 author presentation of Figure 4, see the figure online at http://dx.doi.org/10.1016/j.celrep.2016.10.014#mmc7.

(A and B) Time-lapse images of PD13 zygotes treated with the microtubule-depolymerizing drug MBC. Nuclear oscillations stopped when the loci were paired (A) or unpaired (B); see the schemes on the left. In (A) the loci were mis-segregated and accumulated in one cell pole at meiosis II, although the oscillations resumed and the SPB duplicated normally at meiosis I and meiosis II. Instead in (B), the segregation proceeded normally, similar to untreated cells (see Figures S3A and S3B). Images were acquired at a time interval of 5 min. Time is given in minutes. Loci are highlighted by white arrowheads, and the SPB is indicated by a white asterisk. The white lines mark the cell outline. Scale bar, 2 μm.

(C) Plot of *ade3* loci and SPB position as a function of time corresponding to the experiments shown in (A) and (B) (left and right graphs, respectively). The black dashed line indicates the time during which the oscillations were stopped.

(D) Plot of *ade3* loci distance during the MBC treatment as a function of time, corresponding to the experiments shown in (A) (light blue line, paired) and (B) (dark blue line, unpaired). The gray area indicates the defined pairing distance (400 nm). The average loci distances were 0.21 ± 0.14 μm (paired) and 0.93 ± 0.24 μm (unpaired).

(E) Percentage of PD13 cells with different segregation patterns is plotted for five conditions: untreated control cells, cells where oscillations were stopped with either MBC or TBZ, and loci that were either paired or unpaired, as indicated. In experiments with TBZ the strain PD13C was used. Green, normal segregation; pink, the SPBs were duplicated and all four loci were found close to one cell pole at the end of meiosis I (mis-segregation); gray, SPB and loci in the cell center for more than 2 hr after the oscillations (no segregation). Three different experiments were performed. The number of cells is given in the bars. After the MBC or TBZ washout, about five to seven oscillations were observed. Once the oscillations stopped, the SPB stayed in the center before meiosis I (SPB duplication) for 22.44 ± 7.10 min (control), 26.25 ± 2.58 min (loci paired), and 27.78 ± 5.17 min (loci unpaired), and the difference was not statistically significant (t test, $p_{control/paired} = 0.16$, $p_{control/unpaired} = 0.07$, and $p_{paired/unpaired} = 0.45$).

(F) DNA distribution in the zygotes with segregation problems when the loci were paired (top) and when the loci were unpaired (bottom) during the time when nuclear oscillations were stopped. 1 hr of fixation and DNA staining with Hoechst were performed under the microscope (see the Experimental Procedures) after the time-lapse experiment. From the 35% of cells with mis-segregation problems observed in (D) 2–3 hr after oscillations resumed, seven of ten zygotes showed one single blob of DNA independently of the SPB duplication and three showed a random number of DNA blobs and normal SPB duplication. These three cases could be due to DNA fragmentation caused by the pulling forces exerted by the spindle in the moment of segregation. In the case where the loci were unpaired, they showed four DNA blobs of equal size and normal distribution of SPBs and the loci as described in (D) (n = 15 stained cells from four different experiments).

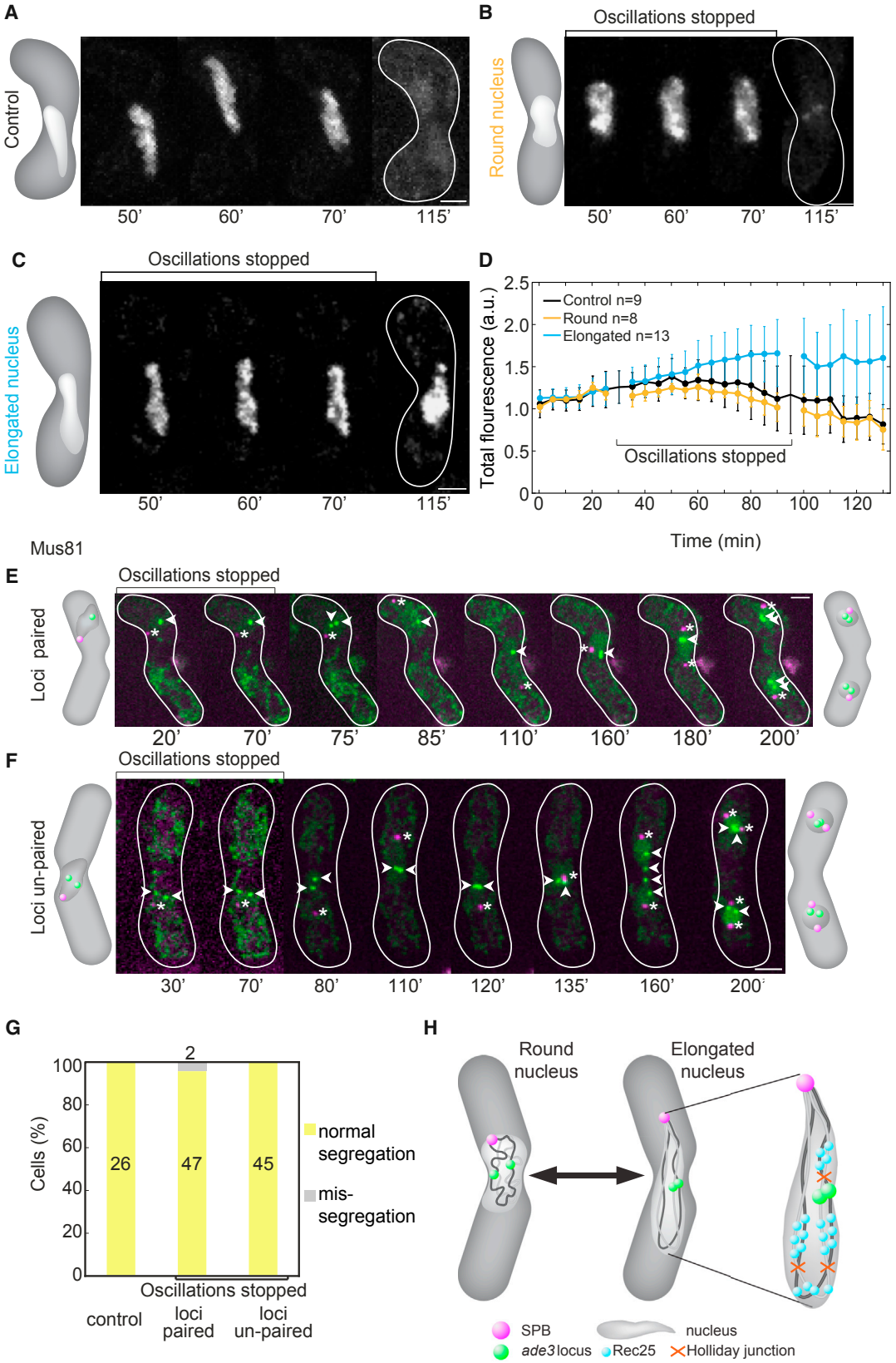

(legend on next page)

It has been suggested that the stretching of the nucleus during the oscillations may further aid chromosome pairing by constantly moving the chromosomes relative to each other (Chikashige et al., 1994). However, this stretching is not permanent because the nuclear shape changes constantly during the oscillations (Yamamoto et al., 1999). Our results show that the nuclear movement is important to maintain the dynamics of pairing and unpairing of homologous loci. Pairing events are more frequent when the SPB is at the cell pole and the nucleus is stretched than when the SPB is in the central region of the cell and the nucleus is roughly round. This relation between the SPB position and the distance between loci depends on the position of the loci. We observed this relation in homologous (*ade3*) as well as heterologous (*ade3*/*cut3*) loci, where both loci are at chromosome arm regions; however, the relation was weak for homologous loci at a centromere-proximal region (*cen2*). At the end of the oscillations, the homologous, but not the heterologous, loci remain paired for a long time. Thus, the dynamics of loci pairing depends on interplay among loci position along the chromosome, sequence homology, and nuclear movement.

These results, together with the observation that the first pairing happens a few minutes after oscillations have started, gave rise to the question, why do the oscillations continue after the pairing has occurred? Simultaneous with chromosome pairing and stabilization by the synaptonemal complex and chiasmata formation, undesirable interactions, such as excessive homologous associations or non-homologous interactions, must be prevented or resolved. Indeed, it has been proposed that nuclear movement takes place in order to avoid unwanted connections and to properly segregate chromosomes at anaphase I (Conrad et al., 2008; Koszul and Kleckner, 2009; Woglar and Jantsch, 2014). In our experiments, pairing events did not last longer than 5 min. However, when oscillations were inhibited and the loci were forced to pair for more than 30 min, the loci remained paired even after the oscillations resumed. In addition, the mis-segreagtion observed after the abrogation of the movement increased when the movement was inhibited at the end of prophase. These findings suggest that there is a maximum duration of chromosome pairing beyond which the dynamics cannot return to normal and that the cell needs a minimum number of oscillations to solve unwanted associations.

Nuclear Movement: A Tool to Dissolve Unwanted Interactions

In addition to excessive recombination between homologous chromosomes, lack of nuclear oscillations may lead to unwanted connections between heterologous chromosomes, which in turn may lead to ectopic recombination. Ectopic recombination was suggested to occur between sequences located on homologous rather than heterologous chromosomes (Goldman and Lichten, 1996). Therefore, a preference of ectopic recombination intermediates toward homologous chromosomes rather than heterologous chromosomes was suggested, indicating that homologous chromosomes have to be closely associated, which is similar to our scenario where we force loci to be paired. It remains an open question whether nuclear movement has a role in keeping heterologous chromosomes apart to inhibit ectopic recombination.

Our experiments have shown that Rec25-GFP accumulates in elongated nuclei when the oscillations are stopped. We propose that stretching of the nucleus and of the chromosomes facilitates loading of Rec25 to the DNA, leading to DSB formation. If this scenario persists for a long time, more irresolvable recombination intermediates may be formed. This hypothesis is supported by our finding that overexpression of the Holliday junction resolvase Mus81 rescues the mis-segregation observed after prolonged pairing. Formation of irresolvable recombination intermediates when oscillations are blocked may be due to additional initiations of recombination or due to conversion of normal recombination events into an irresolvable form.

In conclusion, our results suggest that nuclear oscillations promote dynamic pairing and unpairing of homologous chromosomes, which helps to avoid prolonged chromosome associations. We propose a dual role for nuclear oscillations: enabling

Figure 5. Rec25 Accumulates in Elongated Nuclei and Overexpression of Mus81 Rescues Mis-segregation

(A–C) Time-lapse images of cells expressing Rec25-GFP untreated control (A) or treated with the MT-depolymerizing drug MBC (B and C) during oscillations. Note changes in the nuclear shape. The schemes on the left represent the shape of the nucleus during the time when oscillations were stopped. When the nucleus was elongated (C, up to 70 min), after the oscillations resumed (115 min) there was a high level of fluorescence compared to the same time in (A) and (B). Images were acquired at a time interval of 5 min. Time is given in minutes and the white lines mark the cell outline. Scale bar, 2 μm.

(D) Signal intensity of Rec25-GFP over time. Note that control cells (black line) and cells that are kept with a round nucleus during the treatment (orange line) show a similar fluorescence level. On the contrary, in those cells where the nucleus was elongated (blue line) during the time in which the oscillations were stopped, fluorescence increased and remained at a high level even after the oscillations resumed. We defined round nuclei as those with circularity $\geq$ 0.4, and elongated ones as those with circularity < 0.4 (see the Experimental Procedures and Figure S4B). The difference started to be statistically significant after 70 min ($p_{round/elongated}$ = 0.006). For all the time of the experiment, p values were as follows: $p_{control/round}$ = 0.054, $p_{control/elongated}$ = $4.16*10^{-7}$, and $p_{round/elongated}$ = $1.13*10^{-9}$, t test (n = 30 cells from six different experiments).

(E–G) Overexpression of the Holliday junction resolvase Mus81 rescues the mis-segregation phenotype. Time-lapse images show zygotes overexpressing Mus81 (strain PD13M81), in which the oscillations were stopped by using MBC when the *ade3* loci (arrowheads) were paired (E) or unpaired (F). Note that in both cases the loci segregate normally. Images were acquired at a time interval of 5 min and time is given in minutes. Asterisks mark the SPB and the white lines mark the cell outline. Scale bar, 2 μm. (G) Percentage of cells overexpressing Mus81 that show normal segregation (yellow) and mis-segregation (gray) are quantified. Segregation is plotted for three conditions: untreated control cells, cells where oscillations were stopped by using MBC when *ade3* loci were paired, and cells where oscillations were stopped when *ade3* loci were unpaired. Three different experiments were performed. The number of cells is given in the bars.

(H) Scheme of the dual role for nuclear oscillations. Black arrow denotes oscillations of the nucleus with changes of its shape from a more round to an elongated configuration. Nuclear oscillations are required to induce nuclear stretching in order to promote spatial alignment of chromosomes and to avoid excessive time of chromosome association to ensure a proper segregation. We propose that a certain chromosome configuration, i.e., elongated nucleus, facilitates the loading of the LinE protein Rec25. A prolonged time of nuclear stretching may create an environment in which more Holliday junctions are formed than during normal nuclear dynamics, leading to mis-segregation. SPB, magenta; *ade3* locus, green; nucleus, gray; Rec25, blue; Holliday junction, orange.

spatial alignment of homologous chromosomes for the initial pairing and maintenance of a constant interchange between pairing and unpairing to avoid undesirable connections and mis-segregation.

EXPERIMENTAL PROCEDURES

Strains and Media

Strains of fission yeast used in this study are listed in Table S1. Cells were grown on yeast extract (YE) or Edinburgh minimal medium (EMM) (Forsburg and Rhind, 2006) with appropriate supplements at 25°C ± 0.5°C in a Heraeus incubator (Thermo Scientific).

Construction of Strains

For construction of strain PD13, the strains FY15592 and SI034 (Table S1) were crossed and selected on EMM with G418 (49418.04 Serva) and ClonNat (LEXSY NTC, AB-102, Jena Bioscience). To obtain Movie S1 and Figure 1A, Rec8-GFP- (FY13699, Table S1) labeled cells were crossed with cells labeled for Sid4-mCherry (SI661, Table S1), and zygotes were imaged as described below. To observe heterologous pairing, strains PD05 and PD14 were crossed and meiosis followed under the microscope. Observation of *cen2*-homologous loci was obtained by crossing AK03 and AK04.

Overexpression of either tubulin-mCherry or Mus81 was obtained by transforming PD13 cells via standard transformation procedure with lithium acetate, using 5 μg plasmid DNA. Plasmid pSV01 was generated in the I.M.T. lab and pREP1-RusA was kindly provided by Paul Russel. We selected transformed cells on leu-deficient medium. Cells without the plasmid did not grow on leu-deficient medium (Figure S4C).

Meiosis Induction

In h90 mating-type fission yeast cells, meiosis was induced by suspending a toothpick-full of fresh cells in 50 μL 0.85% sodium chloride (Merck KGaA) and spotting onto malt extract/2% agar (MEA) plates. The plates were then incubated for 6–8 hr at 25°C. For zygotes from cells of opposite mating types (h+ and h−), a half-toothpick of h+ and half-toothpick of h− were suspended in 50 μL 0.85% sodium chloride and spotted onto MEA plates. The plates were then incubated overnight, 12–14 hr, at 25°C. For long time-lapse imaging, a toothpick-full of cells of h90 mating type were added to EMM-N and plated onto glass-bottom dishes for imaging (Forsburg and Rhind, 2006).

Preparation of Cells for Imaging

For imaging, a loopful of cells from the MEA plate was re-suspended in 100 μL EMM-N. The cells were transferred to a lectin-coated (L2380, Sigma-Aldrich), 35-mm, glass-bottom culture dish (MatTek) and allowed to settle for 15 min. Cells were washed with EMM-N and live-cell imaging was performed at 27°C (Bachhoffer chamber). Cells after conjugation and/or karyogamy were detected in bright field, and only synchronized zygotes were selected.

Microscopy

Live-cell imaging was performed on either of the following two microscopes:

(1) Spinning-disk microscope: to observe meiotic prophase in fission yeast zygotes from PD13 and Rec25-GFP (Table S1), an Andor Revolution Spinning Disk system (Andor Technology), consisting of a Yokogawa CSU10 spinning disk scan head (Yokogawa Electric), was employed. The scan head is connected to an Olympus IX71 inverted microscope equipped with a fast piezo objective z-positioner (PIFOC, Physik Instrumente) and an Olympus UPlanSApo 100×/1.4 numerical aperture (NA) oil objective. For GFP excitation, a Sapphire 488-nm solid-state laser (75 mW; Coherent) was used. For mCherry excitation, a 561-nm solid-state Cobolt Jive (75 mW; Coherent) was used. For Hoechst excitation after cell fixation, a standard mercury lamp was used (Olympus). Laser intensity was controlled using the acousto-optic tunable filter in the Andor Revolution laser combiner (ALC, Andor Technology), and it was set according to the fluorescent level of the specimen analyzed, usually 10%–12% of the 488-nm laser and 12%–15% of the 561-nm laser with 0.2 s exposure time. The microscope was equipped with an iXon EM+ DU-897 BV back-illuminated electron multiplying charge coupled device (EMCCD) (Andor Technology). The resulting xy-pixel separation in the images was 168 nm, and the z distance between optical sections was 500 or 600 nm. The system was controlled by Andor iQ software version 1.9.1. The interval between each z stack was 15 s to 5 min. For quantifying fluorescence in Rec25-GFP cells, they were imaged at non-saturated conditions. To avoid fluorescence difference due to the variability of the laser, the laser power was measured with a laser power meter (Gigahertz-Optik) before each experiment and adjusted to 0.0372 W, which usually corresponded to 7%–9% power of the 488-nm laser, and exposure time of 0.15 s for each optical section spanning the entire cell depth. The emission filter used was BL HC 525/30 (Semrock) for GFP and BL HC 605/70 (Semrock) for mCherry. A second spinning disk with similar characteristics was used to simultaneously perform MBC experiments in PD13 zygotes as a control. In this setup, the resulting xy-pixel separation in the images was 162 nm.

(2) Delta vision microscope: to observe meiotic prophase in fission yeast zygotes from PD13 and FY17779, living and fixed cells were imaged on a DeltaVision core microscope, with a motorized XYZ stage (Applied Precision). An Olympus UPlanSApo 100× 1.4 NA oil (R.I. 1.516) immersion objective was used. The illumination was provided by a light-emitting diode (LED) (transmitted light) and Lumicore solid-state illuminator (SSI-Lumencore, fluorescence), and the images were acquired with a Cool Snap HQ2 camera (Photometrics) and the SoftWorx software (Applied Precision), using 2 × 2 pixel binning to minimize light exposure (pixel size = 0.1288 μm). The z distance between optical sections was 500 or 600 nm and the exposure = 0.5 s, 2%–10% transmission, depending on the fluorescent level of the specimen analyzed.

MBC and TBZ Experiments

To stop nuclear oscillations in fission yeast zygotes, we used 25 μg/mL in EMM-N of the microtubule-depolymerizing drug MBC (Carbendazim 97%, Sigma-Aldrich) or 200 μg/mL TBZ (97%, Sigma-Aldrich). To add and wash out the drug while imaging, meiosis was induced in a perfusion chamber (POC-chamber, Helmut Saur). Cells were imaged from karyogamy and, depending on the experiment, MBC or TBZ was added before oscillations started or after several oscillations. MBC or TBZ was left on the cells for 35–60 min and was then washed out with liquid EMM-N, while imaging continued for varying time lengths, to observe the resumption of oscillations and/or meiosis I and meiosis II. For the end point experiments performed in FY17779 and PD13 (Figure S3C), meiosis was induced in a glass-bottom culture dish, and, after zygotes were formed (1–1.5 hr), MBC was added for 1 hr, then washed out, and after 4 hr cells were fixed and DNA stained.

Cell Fixation and DNA Staining

Live-Cell Experiment

To observe the DNA of MBC-treated cells, cells were left for about an additional 4 hr to let them complete meiosis I and meiosis II. Cells were fixed and stained with 4% paraformaldehyde (P6148, Sigma-Aldrich), 0.3% Triton X-100 (X100, Sigma-Aldrich), and 5 μg/mL Hoechst (33342, H1399, Life Technologies) for 10 min. To avoid cell detachment from the dish, the above solution was substituted by 4% paraformaldehyde/5 μg/mL Hoechst in PBS and incubated for about 1–2 hr on the microscope until DNA staining could be observed.

End Point Experiment

Consistent with the live-cell experiments, after 1-hr meiosis induction, cells were treated with MBC for 1 hr and incubated in EMM-N for 4 hr. Then cells were fixed and stained with 4% paraformaldehyde, 0.3% Triton X-100, and 5 μg/mL Hoechst for 10 min. Cells were washed and incubated overnight in mounting medium PBS-80% glycerol/5 μg/mL Hoechst to allow DNA staining. We analyzed zygotes with four spindle pole bodies (indication of the end of meiosis II), and such with visible spores were excluded to ensure they were under MBC treatment.

Cells expressing Rec25-GFP were stained to visualize DNA, after fixation with 4% paraformaldehyde, 0.3% Triton X-100, and 5 μg/mL Hoechst for 10 min.

Image Processing and Data Analysis

To track the position of GFP-tagged loci and the SPB, we used our recently developed algorithm (Krull et al., 2014), optimized for localization of objects with low intensity in settings with high background and noise. We used maximum-intensity projections of z stacks, calculated with ImageJ (NIH). For the measurement of spindle length and thickness, the spindle was detected as an ellipse, and the length and thickness were quantified as the number of fluorescence pixels along the major and the minor axes of the ellipse, respectively. Time 0 was defined as the time frame in which the spindle reached a length of 2.5–3 μm after SPB duplication. To track the shape of the nucleus and fluorescent levels in Rec25-GFP and Rec8-GPF cells, sum-intensity projections were calculated with ImageJ (NIH). These sum projections were converted to binary images, and a mask that exactly matched the contours of the nucleus was constructed for each image; then, the fluorescence level and the circularity were measured using ImageJ plugin circularity = 4 pi(area/perimeter^2). A circularity value of 1 indicates a perfect circle. As the value approaches 0, it indicates an increasingly elongated polygon. The plugin was customized to do the analysis automatically. Final data analysis and statistics were performed using scripts written in MATLAB (MathWorks) and the statistical tool package StatPlus:mac and Microsoft Excel (Microsoft). The ANOVA tests performed were one-way tests. The t tests were two-tailed and two-sample equal-variance tests.

Statistical Analysis

Data are presented as means ± SD from three to ten separate experiments. The significance of data was estimated by Student's t test (two tailed and two sample equal variance) or one-way ANOVA test. Correlation analyses were performed by Pearson correlation coefficient. $p < 0.05$ was considered statistically significant. Values of all significant differences are given with the degree of significance indicated (*$p < 0.05$, ** $p < 0.01$, and *** $p < 0.001$). All parameters were quantified as described in the respective figure legends.

SUPPLEMENTAL INFORMATION

Supplemental Information includes four figures, two tables, and four movies and can be found with this article online at http://dx.doi.org/10.1016/j.celrep.2016.10.014.

AUTHOR CONTRIBUTIONS

I.M.T. conceived and supervised the project. M.R.C. and P.D. designed and performed experiments and analyzed data. All authors discussed the data. M.R.C. and P.D. wrote the paper with contributions from I.M.T.

ACKNOWLEDGMENTS

We thank C. Martin-Castellanos, S. Hauf, and the Yeast Genetic Resource Center for strains; B. Schroth-Diez, D.J. White, and D. Accardi from the Light Microscopy Facility of the Max Planck Institute of Molecular Cell Biology and Genetics (MPI-CBG) for help with microscopy; H. Weisse for technical help; A. Krull, A. Garcia-Ulloa, and D. Ramunno-Johnson for help with image processing and data analysis; V. Zaburdaev, N. Kleckner, V. Ananthanarayanan, T. Franzmann, A. Klemm, and G. Cojoc for fruitful discussions; I. Šarić for the drawings; and the German Research Foundation (DFG, grant SPP1384) for funding. M.R.C. acknowledges support by a Marie Curie Intra-European Fellowship.

Received: April 4, 2016
Revised: July 26, 2016
Accepted: October 4, 2016
Published: November 1, 2016

REFERENCES

Ananthanarayanan, V., Schattat, M., Vogel, S.K., Krull, A., Pavin, N., and Tolić-Nørrelykke, I.M. (2013). Dynein motion switches from diffusive to directed upon cortical anchoring. Cell *153*, 1526–1536.

Bähler, J., Wyler, T., Loidl, J., and Kohli, J. (1993). Unusual nuclear structures in meiotic prophase of fission yeast: a cytological analysis. J. Cell Biol. *121*, 241–256.

Boddy, M.N., Gaillard, P.H., McDonald, W.H., Shanahan, P., Yates, J.R., 3rd, and Russell, P. (2001). Mus81-Eme1 are essential components of a Holliday junction resolvase. Cell *107*, 537–548.

Chikashige, Y., Ding, D.Q., Funabiki, H., Haraguchi, T., Mashiko, S., Yanagida, M., and Hiraoka, Y. (1994). Telomere-led premeiotic chromosome movement in fission yeast. Science *264*, 270–273.

Chikashige, Y., Tsutsumi, C., Yamane, M., Okamasa, K., Haraguchi, T., and Hiraoka, Y. (2006). Meiotic proteins bqt1 and bqt2 tether telomeres to form the bouquet arrangement of chromosomes. Cell *125*, 59–69.

Cojoc, G., Florescu, A.M., Krull, A., Klemm, A.H., Pavin, N., Jülicher, F., and Tolić, I.M. (2016). Paired arrangement of kinetochores together with microtubule pivoting and dynamics drive kinetochore capture in meiosis I. Sci. Rep. *6*, 25736.

Conrad, M.N., Lee, C.Y., Chao, G., Shinohara, M., Kosaka, H., Shinohara, A., Conchello, J.A., and Dresser, M.E. (2008). Rapid telomere movement in meiotic prophase is promoted by NDJ1, MPS3, and CSM4 and is modulated by recombination. Cell *133*, 1175–1187.

Davis, L., Rozalén, A.E., Moreno, S., Smith, G.R., and Martín-Castellanos, C. (2008). Rec25 and Rec27, novel linear-element components, link cohesin to meiotic DNA breakage and recombination. Curr. Biol. *18*, 849–854.

Ding, D.Q., Chikashige, Y., Haraguchi, T., and Hiraoka, Y. (1998). Oscillatory nuclear movement in fission yeast meiotic prophase is driven by astral microtubules, as revealed by continuous observation of chromosomes and microtubules in living cells. J. Cell Sci. *111*, 701–712.

Ding, D.Q., Yamamoto, A., Haraguchi, T., and Hiraoka, Y. (2004). Dynamics of homologous chromosome pairing during meiotic prophase in fission yeast. Dev. Cell *6*, 329–341.

Ding, X., Xu, R., Yu, J., Xu, T., Zhuang, Y., and Han, M. (2007). SUN1 is required for telomere attachment to nuclear envelope and gametogenesis in mice. Dev. Cell *12*, 863–872.

Forsburg, S.L., and Rhind, N. (2006). Basic methods for fission yeast. Yeast *23*, 173–183.

Fowler, K.R., Gutiérrez-Velasco, S., Martín-Castellanos, C., and Smith, G.R. (2013). Protein determinants of meiotic DNA break hot spots. Mol. Cell *49*, 983–996.

Goldman, A.S., and Lichten, M. (1996). The efficiency of meiotic recombination between dispersed sequences in Saccharomyces cerevisiae depends upon their chromosomal location. Genetics *144*, 43–55.

Hiraoka, Y., and Dernburg, A.F. (2009). The SUN rises on meiotic chromosome dynamics. Dev. Cell *17*, 598–605.

Horn, H.F., Kim, D.I., Wright, G.D., Wong, E.S., Stewart, C.L., Burke, B., and Roux, K.J. (2013). A mammalian KASH domain protein coupling meiotic chromosomes to the cytoskeleton. J. Cell Biol. *202*, 1023–1039.

Kakui, Y., Sato, M., Okada, N., Toda, T., and Yamamoto, M. (2013). Microtubules and Alp7-Alp14 (TACC-TOG) reposition chromosomes before meiotic segregation. Nat. Cell Biol. *15*, 786–796.

Keeney, S., Giroux, C.N., and Kleckner, N. (1997). Meiosis-specific DNA double-strand breaks are catalyzed by Spo11, a member of a widely conserved protein family. Cell *88*, 375–384.

Koszul, R., and Kleckner, N. (2009). Dynamic chromosome movements during meiosis: a way to eliminate unwanted connections? Trends Cell Biol. *19*, 716–724.

Koszul, R., Kim, K.P., Prentiss, M., Kleckner, N., and Kameoka, S. (2008). Meiotic chromosomes move by linkage to dynamic actin cables with transduction of force through the nuclear envelope. Cell *133*, 1188–1201.

Krull, A., Steinborn, A., Ananthanarayanan, V., Ramunno-Johnson, D., Petersohn, U., and Tolić-Nørrelykke, I.M. (2014). A divide and conquer strategy for the maximum likelihood localization of low intensity objects. Opt. Express *22*, 210–228.

Labrador, L., Barroso, C., Lightfoot, J., Müller-Reichert, T., Flibotte, S., Taylor, J., Moerman, D.G., Villeneuve, A.M., and Martinez-Perez, E. (2013). Chromosome movements promoted by the mitochondrial protein SPD-3 are required for homology search during Caenorhabditis elegans meiosis. PLoS Genet. *9*, e1003497.

Libuda, D.E., Uzawa, S., Meyer, B.J., and Villeneuve, A.M. (2013). Meiotic chromosome structures constrain and respond to designation of crossover sites. Nature *502*, 703–706.

Lin, Y.T., Frömberg, D., Huang, W., Delivani, P., Chacón, M., Tolić, I.M., Jülicher, F., and Zaburdaev, V. (2015). Pulled polymer loops as a model for the alignment of meiotic chromosomes. Phys. Rev. Lett. *115*, 208102.

Loidl, J. (2006). S. pombe linear elements: the modest cousins of synaptonemal complexes. Chromosoma *115*, 260–271.

Martín-Castellanos, C., Blanco, M., Rozalén, A.E., Pérez-Hidalgo, L., García, A.I., Conde, F., Mata, J., Ellermeier, C., Davis, L., San-Segundo, P., et al. (2005). A large-scale screen in S. pombe identifies seven novel genes required for critical meiotic events. Curr. Biol. *15*, 2056–2062.

Munz, P. (1994). An analysis of interference in the fission yeast Schizosaccharomyces pombe. Genetics *137*, 701–707.

O'Neil, N.J., Martin, J.S., Youds, J.L., Ward, J.D., Petalcorin, M.I., Rose, A.M., and Boulton, S.J. (2013). Joint molecule resolution requires the redundant activities of MUS-81 and XPF-1 during Caenorhabditis elegans meiosis. PLoS Genet. *9*, e1003582.

Parvinen, M., and Söderström, K.O. (1976). Chromosome rotation and formation of synapsis. Nature *260*, 534–535.

Phillips, C.M., Meng, X., Zhang, L., Chretien, J.H., Urnov, F.D., and Dernburg, A.F. (2009). Identification of chromosome sequence motifs that mediate meiotic pairing and synapsis in C. elegans. Nat. Cell Biol. *11*, 934–942.

Rosu, S., Zawadzki, K.A., Stamper, E.L., Libuda, D.E., Reese, A.L., Dernburg, A.F., and Villeneuve, A.M. (2013). The C. elegans DSB-2 protein reveals a regulatory network that controls competence for meiotic DSB formation and promotes crossover assurance. PLoS Genet. *9*, e1003674.

Sato, A., Isaac, B., Phillips, C.M., Rillo, R., Carlton, P.M., Wynne, D.J., Kasad, R.A., and Dernburg, A.F. (2009). Cytoskeletal forces span the nuclear envelope to coordinate meiotic chromosome pairing and synapsis. Cell *139*, 907–919.

Scherthan, H. (2001). A bouquet makes ends meet. Nat. Rev. Mol. Cell Biol. *2*, 621–627.

Scherthan, H., Wang, H., Adelfalk, C., White, E.J., Cowan, C., Cande, W.Z., and Kaback, D.B. (2007). Chromosome mobility during meiotic prophase in Saccharomyces cerevisiae. Proc. Natl. Acad. Sci. USA *104*, 16934–16939.

Sharif, W.D., Glick, G.G., Davidson, M.K., and Wahls, W.P. (2002). Distinct functions of S. pombe Rec12 (Spo11) protein and Rec12-dependent crossover recombination (chiasmata) in meiosis I; and a requirement for Rec12 in meiosis II. Cell Chromosome *1*, 1.

Smith, K.N., Penkner, A., Ohta, K., Klein, F., and Nicolas, A. (2001). B-type cyclins CLB5 and CLB6 control the initiation of recombination and synaptonemal complex formation in yeast meiosis. Curr. Biol. *11*, 88–97.

Tomita, K., and Cooper, J.P. (2006). The meiotic chromosomal bouquet: SUN collects flowers. Cell *125*, 19–21.

Tomita, K., and Cooper, J.P. (2007). The telomere bouquet controls the meiotic spindle. Cell *130*, 113–126.

Tomita, K., Bez, C., Fennell, A., and Cooper, J.P. (2013). A single internal telomere tract ensures meiotic spindle formation. EMBO Rep. *14*, 252–260.

Villeneuve, A.M., and Hillers, K.J. (2001). Whence meiosis? Cell *106*, 647–650.

Vogel, S.K., Pavin, N., Maghelli, N., Jülicher, F., and Tolić-Nørrelykke, I.M. (2009). Self-organization of dynein motors generates meiotic nuclear oscillations. PLoS Biol. *7*, e1000087.

Woglar, A., and Jantsch, V. (2014). Chromosome movement in meiosis I prophase of Caenorhabditis elegans. Chromosoma *123*, 15–24.

Woglar, A., Daryabeigi, A., Adamo, A., Habacher, C., Machacek, T., La Volpe, A., and Jantsch, V. (2013). Matefin/SUN-1 phosphorylation is part of a surveillance mechanism to coordinate chromosome synapsis and recombination with meiotic progression and chromosome movement. PLoS Genet. *9*, e1003335.

Wynne, D.J., Rog, O., Carlton, P.M., and Dernburg, A.F. (2012). Dynein-dependent processive chromosome motions promote homologous pairing in C. elegans meiosis. J. Cell Biol. *196*, 47–64.

Yamamoto, A., West, R.R., McIntosh, J.R., and Hiraoka, Y. (1999). A cytoplasmic dynein heavy chain is required for oscillatory nuclear movement of meiotic prophase and efficient meiotic recombination in fission yeast. J. Cell Biol. *145*, 1233–1249.